Investigation of the Impact of Powder Shape on Spreading Dense Layers Using the Spreading Tester

Marco Mitterlehner[1,2], Harald Gschiel[1], Herbert Danninger[2], and Christian Gierl-Mayer[2]

[1]voestalpine Böhler Edelstahl GmbH & Co KG, Kapfenberg, Austria
[2]Institut für Chemische Technologien und Analytik, TU Wien, Vienna, Austria

Abstract: In Laser Beam Powder Bed Fusion (LB-PBF) technologies, spreading of powder layers as dense and as fully covered as possible is of crucial importance for a good processability of powders. Poorly covered layers or layers with undesirable features in it, such as elongated, powderless craters in the direction of spreading, might result in defective printed parts. The reason for this could be either poor powder quality or a poorly adjusted build job. To investigate the surface coverage of a single spread powder layer, a new method was developed using the Spreading Tester. With this, two powder grades differing mostly in their particle shape were used to investigate the impact of powder shape on the surface coverage.

Keywords: Additive Manufacturing, Laser Beam Powder Bed Fusion, IN718, Particle shape, Sphericity, Spreadability, Testing, Python

Untersuchung des Einflusses der Partikelform auf den Auftrag dichter Schichten mit dem Spreading Tester

Zusammenfassung: Bei Laser Beam Powder Bed Fusion (LB-PBF)-Technologien ist das Auftragen von möglichst dichten und vollständig bedeckten Pulverschichten von entscheidender Bedeutung für eine gute Verarbeitbarkeit von Pulvern. Schlecht bedeckte Schichten oder Schichten mit unerwünschten Merkmalen, wie beispielsweise länglichen, pulverlosen Kratern in Ausbreitungsrichtung, können zu fehlerhaften Bauteilen führen. Der Grund dafür könnte entweder eine schlechte Pulverqualität oder ein schlecht eingestellter Druckjob sein. Zur Untersuchung der Oberflächenabdeckung einer einzelnen aufgetragenen Pulverschicht wurde eine neue Methode mit dem Spreading Tester entwickelt. Dabei wurden zwei Pulversorten verwendet, welche sich hauptsächlich in ihrer Partikelform unterscheiden, um den Einfluss der Pulverform auf die Oberflächenabdeckung zu untersuchen.

Schlüsselwörter: Additive Fertigung, Laser Beam Powder Bed Fusion, IN718, Partikelform, Sphärizität, Rakelfähigkeit, Prüfen, Python

1. Introduction

The characteristic element of LB-PBF Additive Manufacturing (AM) technologies is the layer-by-layer build-up of the products. As a result, these technologies have a high degree of design freedom, which means that special features, such as internal cooling channels or surface-optimized components, can be produced that cannot be realized using conventional manufacturing methods. A major disadvantage of the AM technologies, however, is the very time-consuming production process. It is therefore all the more important that the powder used for production is tested in advance to check its suitability for the respective AM process. Currently, however, there are no corresponding standards for this purpose, which is why standards from the field of powder metallurgy are used instead. It should be noted here that some standard test methods, such as those for measuring the flow time with a so-called Hall funnel, are not well suited for powders used in this field, since they do not reflect the AM process well enough. For this reason, interest in the study of spreading powder layers in this community has increased in recent years. The suitability of a powder to be spread in the form of an exceptionally thin, particularly uniform and as dense as possible layer is also called spreadability. There are already several different approaches to characterize powders for this field [1–4], e.g. using a powder rheometer. Some studies are also already investigating the spreadability itself and contain test series aimed at investigating the influences of various process parameters on spreading of powder layers [5–15].

Looking at the process of spreading powder layers in LB-PBF AM technologies in detail, a distinction can be made be-

M. Mitterlehner (✉)
voestalpine Böhler Edelstahl GmbH & Co KG,
Kapfenberg, Austria
marco.mitterlehner@voestalpine.com

Fig. 1: Spreading Tester
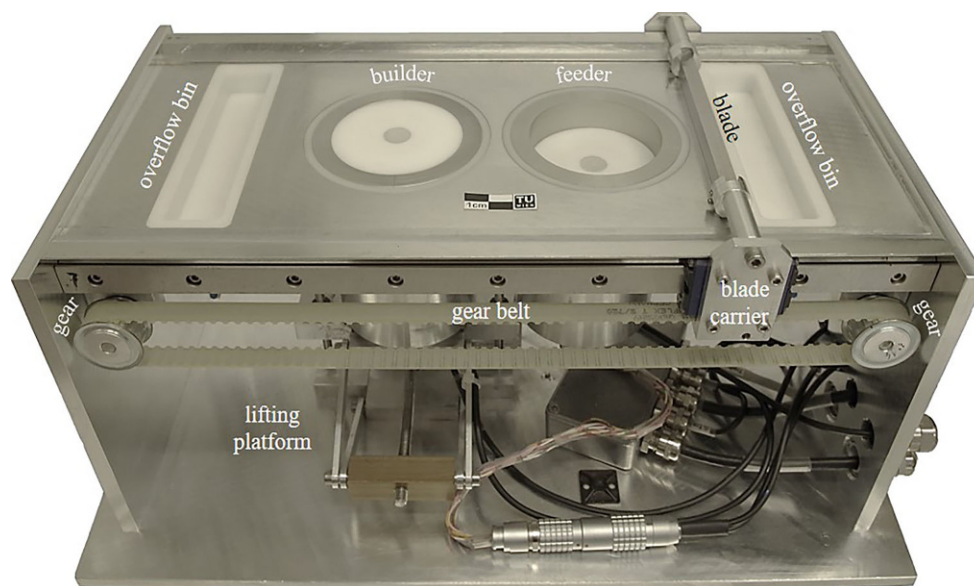
tween two fundamentally different processes: Firstly, that in which the new powder layer is spread on the loose powder bed and, secondly, that in which the powder is spread on already melted material from the underlying layer, i.e. on top oft he built specimen. Both types of spreading can be investigated with the so-called Spreading Tester already presented e.g. in [13] and described in more detail in [16]. For the present study, however, the focus was exclusively on spreading of powder layers on already melted material.

2. Experimental Procedure

2.1 Powders Used and Basic Powder Characterization

Two different grades of IN718 superalloy powder in the particle size range of approximately 15 to 53 μm were used as base powders for this study, differing mainly in shape. One was produced by inert gas atomization and therefore has basically a spherical shape, but also contains some satellites and agglomerates (see Fig. 8). The other was produced by inert gas atomizing with subsequent plasma spheroidization and therefore contains almost uniformly highly spherical particles. Two further blends were prepared from these powders, one using 25 and one using 50 wt% of the plasma spheroidized powder, the balance being the just atomized one. Thus, a total of four different powder grades were used for this study.

Using the original powders as well as the powder blends, a basic powder characterization was performed by determining the Hall flow rate according to [17], the apparent density using a funnel according to [18] as well as an Arnold Meter according to [19] and the tap density according to [20]. Additionally, a CAMSIZER X2 with its default settings was used to measure the volume-related sphericity (SPHT3) as well as the volume-related particle size distribution (PSD), whereby the minimum chord length ($x_{c,\,min}$) was

chosen for the determination of the particle size of a single particle, and the class width was set to 1 μm. The powders were also investigated using a JEOL JSM 6490 HV scanning electron microscope (SEM).

2.2 Spreading Tester

Since there are no standardized test methods for testing the spreadability of a powder, a special testing device was developed for this purpose—the so-called Spreading Tester (Fig. 1). This tester is a miniature 3D printer that is not equipped with a laser, operates in ambient air and is therefore only used to test powders for use in LB-PBF technologies, such as selective laser melting (SLM). With the help of this device, previously unexplored phenomena can now be investigated in more detail. The Spreading Tester is controlled via a self-written LabVIEW program, which makes it possible to vary a large number of parameters for a single experiment. These include, for example, the layer thickness, the spreading velocity of the powder using the recoater blade, or the number of layers spread. It is also possible to choose between different spreading strategies. More precisely, this is the chronological order of the individual process steps when spreading the powder. In addition to these software settings, hardware settings can also be changed, such as the so-called gap size, which corresponds to the distance between the recoater blade and the building platform. This is adjusted before each experiment and can be individually adapted to a desired value using a feeler gauge. The recoater blade itself can also be changed, for which a simple attachment enables using use polymer recoater blades with a wide variety of shapes in addition to a recoater blade made of HSS with a rhombic shape. A selection of different recoater blades as well as a sketch of the attachment for mounting polymer recoater blades are shown in Fig. 2.
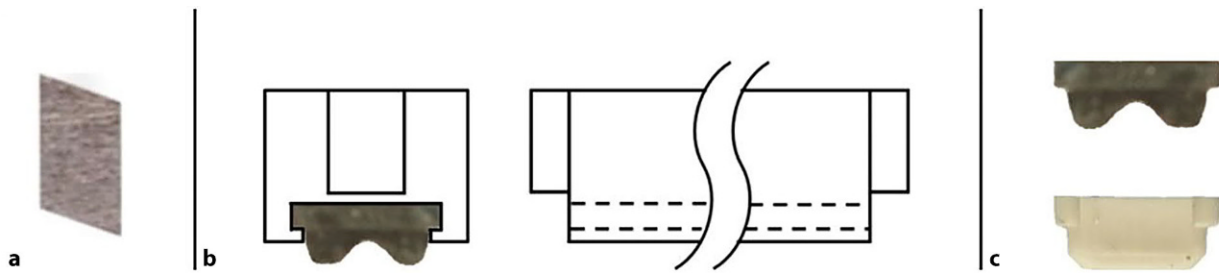
Fig. 2: HSS recoater blade (**a**), attachment to mount polymer re-coater blades (**b**), and two mountable polymer recoater blades (**c**)

In addition to the Spreading Tester itself, various methods for examining spread powder layers have also been developed. One method is used to determine the surface roughness of the top spread powder layer. For this purpose, several powder layers are spread on the builder and then the top spread powder layer is imaged three-dimensionally and examined. Another method determines the powder bed density after spreading a defined number of powder layers. The mass of the spread powder is simply weighed and the volume of the builder in which the powder was spread is taken from the controlling software, thus providing all the information required for the calculation. The last method is about measuring the surface coverage of a single spread powder layer. Since only the last-mentioned method is of interest for this study, it is explained in more detail in the following.

2.3 Evaluating the Surface Coverage of a Single Spread Powder Layer

In [13] a method for measuring the surface coverage of a single spread powder layer using the Spreading Tester has already been introduced. This mimics spreading powder on already melted material on the underlying layer in the real printing process. However, if the standard builder of the Spreading Tester is used, inaccuracies can occur. This is mainly due to the fact that the builder, or rather the surface on which the single powder layer is spread, consists of several individual parts, which furthermore are partly movable. In order to improve the reproducibility and significance of the results, this method has been further developed. In order to better understand the advances of the newly developed method, the original method will nevertheless be explained very briefly:

First, the builder was positioned in the Spreading Tester, the building platform was moved to its top position and the gap size was adjusted with the help of a feeler gauge. Then the recoater blade was initialized and positioned to the right of the feeder (referring to Fig. 1). Then the feeder was filled with powder, and the piston in it was moved upwards by the desired amount to provide powder for the upcoming test. Then the desired spreading velocity was set and finally the recoater blade was moved forward until behind the builder, depositing one single layer on it. This resulting spread powder layer was then three-dimensionally imaged using a Keyence VHX-5000 digital microscope at 800x magnification on nine different spots located at the same position in each experiment. The images were stitched from 5 × 6 single images, which resulted in the size of a stitched image being approximately 1.1 × 1.1 mm. The height of each pixel was then extracted from the stitched three-dimensional image and was transferred to a two-dimensional matrix. The height data from this matrix were then plotted, revealing two peaks: one for the empty spaces between the particles at lower height values, which could be assigned to the building platform, and one for the particles themselves at higher height values. It should be mentioned that the microscope software slightly smoothened the three-dimensional surface, which meant that the transition of the height between the particles and the building platform was, on the one hand, gradual instead of abrupt and, on the other hand, not precise. In the end, two peaks were fitted into the plotted height data, and the area underneath each peak was determined. The proportion of the area of the peak assigned to the particles then corresponded to the surface coverage.

In order for this method to ensure that the building platform was always at the same height during a test series and that it always had the same inclination, since it has a certain amount of clearance in the builder to be able to move up and down, it was moved to its top position before a test series was carried out and was then not moved again for the entire test series.

For the further development of this method, the most important step was to replace the builder with a dummy. After several approaches, the following one turned out to be

Fig. 3: Dummy for measuring the surface coverage of a single spread powder layer

the most promising one. The dummy developed consists of two separate parts and can be seen in Fig. 3.

The more important part, on which the single powder layer will later be spread, is the upper one. This is made of an AlMgSi1 alloy, which has been turned after the shape of the builder in order to fit into the Spreading Tester. A special feature of the dummy is that the surface on which the powder layer is to be spread was ground and polished to a mirror finish after turning to remove the pattern on the surface created by turning, and this surface was then anodized red. Due to the red color, the background strongly contrasts in color against the grey powder particles lying on it when the spread powder layer is investigated later. This type of production gives the surface a certain roughness, but it still remains flat. The surface roughness value (R_a) is 0.45 µm. This value is around one order of magnitude lower than that of a surface melted using an LB-PBF AM technology, such as SLM, on which the next powder layer is then spread [21]. However, it is still a decent approximation of spreading powder on previously melted material from the underlying layer like in the real printing process.

The lower part of the dummy consists of a turned red PVC cylinder, which makes the dummy light enough to be placed on the stage of the digital microscope for the evaluation. The two individual parts are connected to each other in a non-twisting way, and the dummy can only be placed in the same way and orientation in the Spreading Tester as well as on the microscope stage due to its special design.

To measure the surface coverage of a single spread powder layer, the dummy is first placed in the Spreading Tester, and the gap size is adjusted with the help of a feeler gauge. The recoater blade is then initialized so that it is located to the right of the feeder (referring to Fig. 1). Now the feeder is filled with powder, the piston inside it is lifted to provide powder for spreading, and then the recoater blade is moved forward until behind the dummy, coating it with a single powder layer. Before the dummy can be removed, the interface between the dummy and the stage of the Spreading Tester is carefully cleaned with a brush without changing the center of the spread powder layer, which will be used for examination. This prevents powder from dropping down

into the electronics of the Spreading Tester through the gap between the dummy and the Spreading Tester when the dummy is removed. The dummy is then elevated using the lifting platform of the Spreading Tester, carefully removed from it, transported with utmost care to a Keyence VHX-5000 digital microscope next door, and placed on the stage of the digital microscope. It has already been investigated in [16] that the spread powder layer is not changed during the careful transport. Now, three-dimensional images of the powder layer are taken at 200x magnification of only four different spots, which are at the same positions for each experiment due to a special procedure. These images are stitched from 7 × 9 single images each and thus have a size of approximately 8.25 × 8.25 mm.

For further evaluation of the images, the three-dimensional information of the images is now discarded and only the crisp two-dimensional images are used. For this purpose, an algorithm was written in Python 3.5 using the OpenCV module, which in principle just distinguishes between the particles and the dummy surface, which mimics the already melted material of the underlying layer. For this purpose, such an image is first loaded into the computer's memory and then converted from the RGB color space into the HSV color space so that it can be processed using the desired module. In advance, the HSV color segments that can be assigned to the dummy were determined and preselected on the basis of several images. Thus, all pixels the HSV values of which are in the range of the preselected color segments are detected in the image and selected. The position of these pixels is stored in a separate matrix, which is now used to create a simple black-and-white image. This conversion step is illustrated by a small, magnified section of an image of a single powder layer that was spread using 60 µm gap size and 50 mm/s spreading velocity in Fig. 4. Finally, by determining the percentage of black pixels in the black-and-white image, the surface coverage can be determined. The surface coverage for the example of the magnified section shown in Fig. 4 is 58.1%.

The further development of this method thus offers several advantages. On the one hand, the real printing process is reflected better, since powder is spread on a rough sur-

Fig. 4: Evaluation of a crisp two-dimensional image—original image (**a**) and corresponding black-and-white image (**b**)
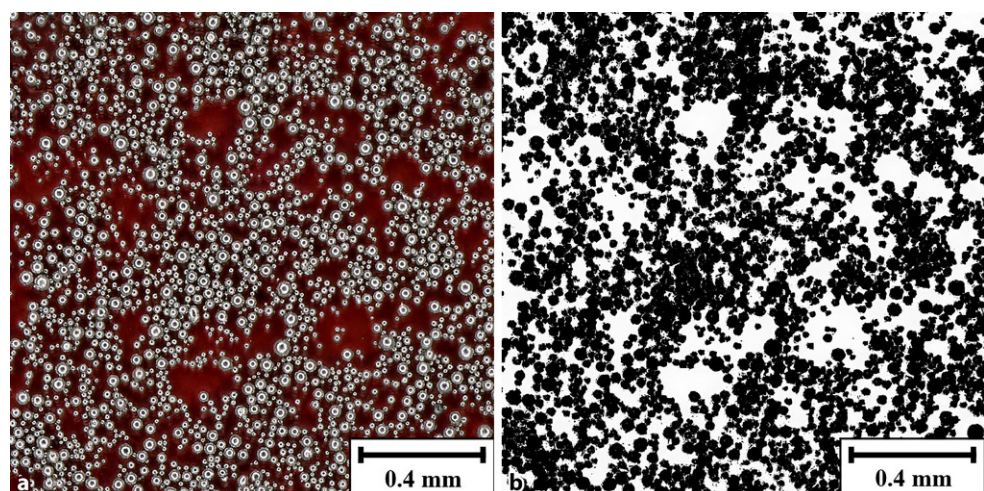
face like the already melted material from the underlying layer. On the other hand, the three-dimensional height data are not required, which eliminates the inaccuracies caused by the smoothening of the surface by the microscope software and the necessary fit. Furthermore, since, instead of the accurate height data of each pixel, only the sharp two-dimensional image is needed for the evaluation, the resolution of the images can be reduced. In several tests, therefore, the new settings described above were evaluated for taking the images on the microscope, where the resolution is lower but still sufficient for evaluation. All this results in the fact that, compared to the previous method for evaluating the surface coverage of a single spread layer, the investigated area could be significantly enlarged (approx. 25 times larger) and the examination could still be accelerated (approx. 3.75 times faster).

2.4 Performing an (Approximately) Uniform Printing Process

Considering the start of the printing process with the first spreading and then selectively melting the first powder layer at the height of the initial gap size (δ_{init}), the voids between the particles cause the selectively melted material to densify and shrink, as can be seen in Fig. 5. This compaction can be described using Eq. 1, where f_M is the fraction of the material (=powder).

Equation 1: Formula for calculating the densification of the powder bed by selective melting in the first powder layer

$$h_{M, init} = \delta_{init} \cdot f_M \qquad (1)$$

By considering this densification, a condition can be derived for an approximately uniform production throughout. Namely, in order to spread exactly the same amount of powder over the already melted material in the next layer, the building platform has to be lowered by a precisely defined amount corresponding to the height of the densified material ($h_{M, init}$), as shown in Fig. 6.

Thus, $d_l = h_{M, init}$ applies, where d_l is the layer thickness. If this condition is inserted into Eq. 1 and the assumption is made that the fraction of the ρ_M powder (f_M) corresponds to the ratio between the apparent density measured using an Arnold Meter (AD_{AM}) and the density of the (melted)
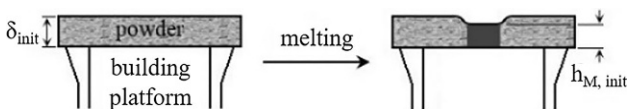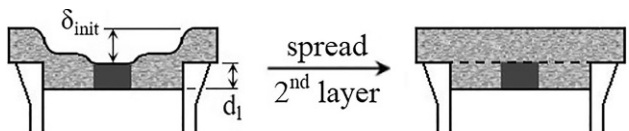
material (ρ_M), the relationship between the layer thickness and the initial gap size given in Eq. 2 is obtained. For this purpose, the apparent density measured by means of an Arnold meter is used, since this measurement method reflects the LB-PBF process much better than the one with a Hall funnel. With this equation, the ideal layer thickness for the printing process can be calculated and set with a known initial gap size.

Equation 2: Formula for calculating the ideal layer thickness (d_l) for an approximately uniform printing process

$$d_l = \delta_{init} \cdot AD_{AM} \qquad (2)$$

It should be noted that spreading powder layers that are not completely homogeneous or covered also influences the relationship given in Eq. 2 and can thus lead to a nonuniform printing process. However, this should not be part of the results shown and discussed here.

2.5 Tests Performed

For this study, the influence of the particle shape on the surface coverage was investigated in a first trial using the four different powder variants—two plain powders and two mixtures—and the further developed method for measuring the surface coverage of a single spread powder layer. In addition, an attempt was made to determine the initial gap size for the powder variants used at which the surface coverage is approximately 100%. For this purpose, several experiments were carried out in which the gap size was increased from 50 µm to a maximum gap size of 100 µm—as this was the thickest available feeler gauge—in 10 µm steps, and a spreading velocity of 150 mm/s was used.

3. Experimental Results and Discussion

3.1 Basic Characteristics of the Powders Used

In Fig. 7 the volume-related particle size distribution (PSD) of both unmixed base powders are shown. It can be seen that the PSD of the plain inert gas atomized powder does not differ greatly from that of the subsequently plasma
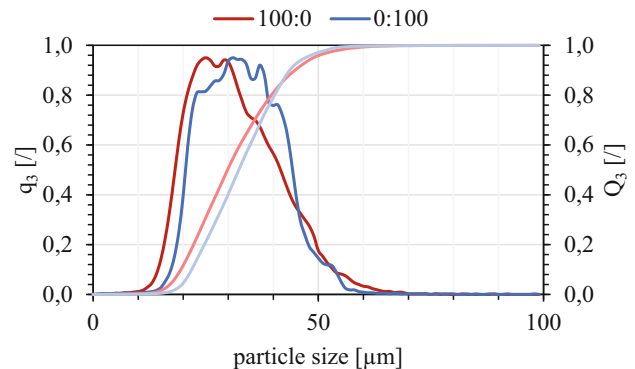
Fig. 5: Densification of melted powder

Fig. 6: Approximately uniform printing process

Fig. 7: Volume-related PSD of the unmixed powders (100:0 ≙ inert gas atomized; 0:100 ≙ plasma spheroidized)

TABLE 1 Volume-related characteristic d-values ($d_{10, 3}$, $d_{50, 3}$, $d_{90, 3}$) and sphericity (SPHT3) of all powder variants used				
Mixing ratio [inert:plasma]	$d_{10, 3}$ [µm]	$d_{50, 3}$ [µm]	$d_{90, 3}$ [µm]	SPHT3 [/]
100:0	20.5	30.8	45.8	0.8854
75:25	20.8	32.0	46.5	0.9068
50:50	21.1	33.3	46.8	0.9274
0:100	22.9	33.3	44.6	0.9674

spheroidized powder. The PSD of the plain inert gas atomized powder is even slightly shifted towards smaller particle diameters in comparison. Thus, the results obtained in this study can, in a first approximation, be attributed to the influence of particle shape. In addition, Table 1 shows volume-related characteristic d-values of all powder variants as well as their sphericity value. This again confirms the similarity of the PSDs. It also shows the required increase in the sphericity of the powder variants from the inert gas atomized to the subsequently plasma spheroidized powder.

Fig. 8 shows the SEM images of both base (unmixed) powders used. It can be seen that the particles in the inert gas atomized powder (Fig. 8a) have a basically spherical shape, but the powder also has agglomerates, irregular-shaped particles, and satellites adhering to larger particles. The subsequently plasma spheroidized powder (Fig. 8b), on the other hand, contains almost exclusively perfectly spherical particles. Only very few satellites can be seen in it.

In Table 2 the basic powder characteristics are listed. All values shown are an average of three single measurements. It can be seen that the plain inert gas atomized powder and the 75:25 powder mixture did not flow through the Hall funnel. Furthermore, these two did not even flow through the Carney funnel with an orifice twice as large, which is why the apparent density determined by means of a funnel is not given. The 50:50 powder mixture as well as the plain plasma spheroidized powder, on the other hand, even flowed through the Hall funnel. In general, the table also clearly shows the influence of the particle shape on the powder characteristics, whereby these also improve continuously with increasing sphericity of the particles.

3.2 Evaluating the Surface Coverage of a Single Spread Powder Layer

In Fig. 9 the measured surface coverage of a single spread powder layer is shown for all experiments with a spreading speed of 150 mm/s, different gap sizes from 50 to 100 µm in 10 µm steps, and all four powder variants. Since each value is an average of four measurement points, the corresponding standard deviation of these values is also given in Fig. 9. Once more it should be pointed out that spreading powder on already melted material from the underlying
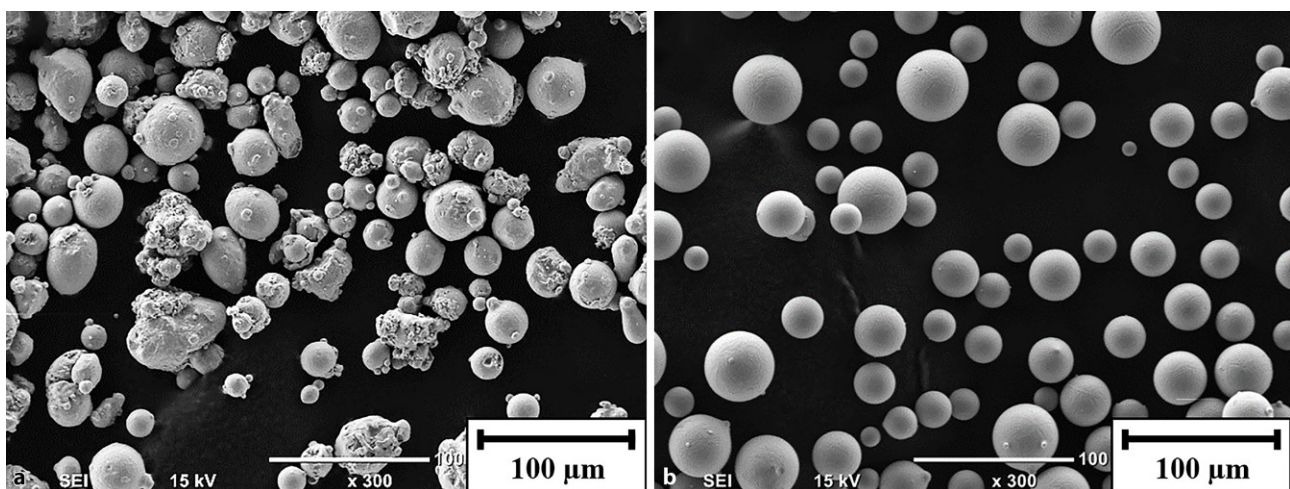

Fig. 8: SEM images of both unmixed powders (**a** inert gas atomized, **b** plasma spheroidized)

TABLE 2 Basic powder characteristics of all powder variants used				
Mixing ratio [inert:plasma]	FT [s/50 g]	AD_F [g/cm³]	AD_{AM} [g/cm³]	TD [g/cm³]
100:0	Not measurable	Not measurable	4.00 ± 0.02	4.75 ± 0.01
75:25	Not measurable	Not measurable	4.18 ± 0.02	4.86 ± 0.03
50:50	13.5 ± 0.1	4.21 ± 0.01	4.36 ± 0.01	4.91 ± 0.04
0:100	10.1 ± 0.1	4.67 ± 0.02	4.83 ± 0.01	4.96 ± 0.01
FR flow rate, *AD_F* apparent density measured using a funnel, *AD_{AM}* apparent density measured using an Arnold Meter, *TD* tap density				

150 mm/s	mixing ratio [inert:plasma]			
	100:0	75:25	50:50	0:100
50	8.7 ± 1.5	8.1 ± 0.6	26.4 ± 1.7	35.4 ± 0.8
60	12.3 ± 3.3	24.4 ± 1.1	34.9 ± 1.1	37.3 ± 1.8
70	17.0 ± 1.3	37.9 ± 2.8	57.9 ± 5.3	66.3 ± 2.1
80	30.3 ± 6.9	49.4 ± 1.6	66.4 ± 3.5	72.2 ± 1.0
90	44.3 ± 1.3	57.6 ± 3.3	72.5 ± 1.9	88.5 ± 0.8
100	53.3 ± 3.8	67.4 ± 1.6	82.9 ± 1.0	95.8 ± 0.6

(gap size [µm] on vertical axis)

Fig. 9: Surface coverage of a single spread powder layer for all experiments

layer is mimicked here. Two fundamental findings can now be obtained from these data.

Firstly, it is evident that the surface coverage increases with an increasing gap size, independently of the powder variant used and thus also independent of the particle shape. This is obviously due to the fact that the larger the gap between the recoater blade and the already melted material of the underlying layer, the more powder particles can pass through this gap and thus the surface coverage is larger.

Secondly, it is also evident that the surface coverage also increases with increasing sphericity, independently of the gap size used. This means that irregularly shaped particles are less able to pass through the gap between the recoater blade and the already melted material of the underlying layer compared to spherical particles of more or less the same size. It should also be highlighted here that the plain inert gas atomized powder is slightly shifted towards smaller particle diameters, as shown in Fig. 7. If it is assumed that both plain powders have the same sphericity, the finer powder would lead to a more completely covered layer using the same gap size as the particles can pass through the gap more easily. However, since the sphericity differs and the slightly coarser plain plasma spheroidized powder with a higher sphericity has the higher surface coverage, the strong influence of the particle shape is once again evident here.

Another fact that can be derived from these data is that the different powder variants need not flow through either the Hall funnel (or the Carney funnel, with an orifice twice as large) in order to be spread without any problems. This once more confirms that the Hall flow rate is not a significant parameter for assessing the spreadability of a powder for AM.

Since the thickest feeler gauge available for setting the gap size for the experiments was 100 µm, it was not possible to spread a 100% covering powder layer for the powder variants used as can also be seen in Fig. 9. The best result was obtained with the plain plasma spheroidized powder, with which a surface coverage of 95.8% could be achieved at a spreading velocity of 150 mm/s and a gap size of 100 µm. Nevertheless, in order to calculate the ideal layer thickness for an approximately uniform printing process it is now ten-

tatively assumed that the surface coverage was 100% in this experiment. Thus, the initial gap size is 100 µm. According to Table 2, the apparent density measured by an Arnold Meter is 4.96 g/cm³ and the nominal material density of IN718 according to its datasheet is 8.20 g/cm³. If these data are now inserted into Eq. 2, an ideal layer thickness of 58.9 µm results, which is the value by which the building platform has to be lowered for a subsequent, approximately uniform printing process using the plain plasma spheroidized powder.

4. Summary

In this study, a new method for measuring the surface coverage of a single spread powder layer was introduced. In this process, spreading powder on already melted material from the underlying layer is mimicked in the real printing process. Compared to the previous method presented in [13], it was possible to accelerate the execution of the measurement, to increase the area investigated, and to improve the accuracy and reproducibility of the results obtained. In addition, the mimicking of the real printing process was improved as the single powder layer is now spread on a slightly rough surface similar to a printed one.

Due to the fact that the two plain base powders had a very similar particle size distribution, the influence of the particle shape could be investigated in the best possible way in this study. It was observed that, as the sphericity increased, the powder characteristics improved, due to better space occupancy and less risk of particles becoming entangled with each other during movement. In addition, the surface coverage of a single spread powder layer also increased with an increasing sphericity. This means that non-spherical particles experience more difficulty in passing through a gap of the same size than spherical ones, when being spread on already melted material from the layer below, which might differ when spreading on a loose powder bed. It was also observed that, as the gap size increased, so did the surface coverage of a single spread powder layer as more particles could simply pass through the larger gap.

A condition was also presented with which an approximately uniform printing process can be carried out in which the spread powder layers show 100% coverage. It was shown which data are required for this and how it can be obtained. Finally, the ideal layer thickness could be calculated as an approximation, at least for the plain plasma spheroidized powder.

Once more it was shown that it is not necessary for powder to flow freely through the Hall or even the Carney funnel in order to be spread without any problems in an LB-PBF technology.

References

1. Hare, C., Zafar, U., Ghadiri, M.: Analysis of the dynamics of the FT4 powder rheometer. Powder Technol. **285**, 123–127 (2015)
2. Lumay, G., Boschini, F., Traina, K.: Measuring the flowing properties of powders and grains. Powder Technol. **224**, 19–27 (2012)
3. Anton Paar: Powder rheology. https://wiki.anton-paar.com/en/powder-rheology/, Accessed 4 July 2021
4. Microtrac Retsch: Ensuring high quality in the additive manufacturing process. https://www.microtrac.de/dltmp/www/5e396c14-fe94-4af0-83c0-7f30c3c9c754-49caf39811f8/tr_additive_manufacturing_vs_0519_en.pdf, Accessed 1 July 2020
5. Parteli, E.J.R., Pöschel, T.: Particle-based simulation of powder application in additive manufacturing. Powder Technol. **288**, 96–102 (2016)
6. Jacob, G., Brown, C.U., Donmez, A.: The influence of spreading metal powders with different particle size distributions on the powder bed density in laser-based powder bed fusion processes. US Department of Commerce, National Institute of Standards and Technology (2018)
7. Mitterlehner, M., Danninger, H., Gierl-Mayer, C.: Study on the layer building of powders in powder bed fusion processes for additive manufacturing. In: Proceedings Euro PM2018 Congress & Exhibition, Bilbao. European Powder Metallurgy Association (EPMA), Shrewsbury (2018). ID 3988826
8. Mitterlehner, M., Danninger, H., Gierl-Mayer, C.: A new method for describing the morphology of powder layers in direct laser melting. In: Proceedings 3rd Metal Additive Manufacturing Conference 2018, Vienna, p. 31–40. Austrian Society for Metallurgy and Materials (ASMET), Leoben (2018)
9. Nan, W., Pasha, M., Bonakdar, T.: Jamming during particle spreading in additive manufacturing. Powder Technol. **338**, 253–262 (2018)
10. Alchikh-Sulaiman, B., Carriere, P.R., Chu, X.: Powder spreading and tribocharging for additive manufacturing process. Proceedings Euro PM2019 Congress & Exhibition, Maastricht. European Powder Metallurgy Association (EPMA), Shrewsbury (2019). ID 4347446
11. Gopaluni, A., Lyckfeldt, O., Hatami, S.: Powder spreadability in metal additive manufacturing. Paper presented at: Alloys for Additive Manufacturing Symposium 2019, Gothenburg. CAM2—Centre for Additive Manufacturing—Metal, Gothenburg (2019)
12. Schrage, J., Schleifenbaum, J.H.: Influence of powder application parameters on powder bed properties and on productivity of laser powder bed fusion (L-PBF). Proceedings 4th Metal Additive Manufacturing Conference 2019, Örebro. Austrian Society for Metallurgy and Materials (ASMET), Leoben, pp. 28–37 (2019)
13. Mitterlehner, M., Danninger, H., Gierl-Mayer, C.: Study on the influence of the blade on powder layers built in powder bed fusion processes for additive manufacturing. Berg. Huettenmaenn. Monatsh. **165**(3), 157–163 (2020)
14. Mitterlehner, M., Danninger, H., Gierl-Mayer, C.: Spreading behaviour and packing density of the powder bed in L-PBF as a function of spreading strategy and velocity. In: Proceedings Euro PM2020 Virtual Congress & Exhibition, Virtual. European Powder Metallurgy Association (EPMA), Shrewsbury (2020). ID 4854670
15. Mitterlehner, M., Danninger, H., Gierl-Mayer, C.: Investigation of the influence of powder moisture on the spreadability using the spreading tester. Berg. Huettenmaenn. Monatsh. **166**(1), 14–22 (2021)
16. Mitterlehner, M.: Metal powders for laser powder bed fusion technologies: storing, drying, spreading, printing. PhD Thesis. Technische Universität Wien (TU Wien), Vienna (2020)
17. ISO/TC 119/SC 2, "Metallic powders—Determination of flow rate by means of a calibrated funnel (Hall flowmeter)", International Organization for Standardization (ISO), Vernier, Switzerland (2018), Standard No. 4490:2018.
18. ISO/TC 119/SC 2, "Metallic powders—Determination of apparent density—Part 1: Funnel Method", International Organization for Standardization (ISO), Vernier, Switzerland (2018), Standard No. 3923–1:2018.
19. B09.02, "Standard Test Method for Apparent Density of Metal Powders and Related Compounds Using the Arnold Meter", American Society for Testing and Materials International (ASTM International), West Conshohocken, Pennsylvania (2017), Standard No. B703–17.
20. ISO/TC 119/SC 2, "Metallic powders—Determination of tap density", International Organization for Standardization (ISO), Vernier, Switzerland (2018), Standard No. 3953:2011.
21. Mitterlehner, M., Danninger, H., Gierl-Mayer, C.: Processability of Moist Superalloy Powder by SLM. Berg. Huettenmaenn. Monatsh. **166**(1), 23–32 (2021)